Mixed Phosphathia Macrocyclic Chemistry: Synthesis and Characterisation of $[M(Ph_2[14]aneP_2S_2)]^{2+}$ (M = Pd or Pt) and $[RhCl_2(Ph_2[14]aneP_2S_2)]^+$ ($Ph_2[14]aneP_2S_2$ = 8,12-Diphenyl-1,5-dithia-8,12-diphosphacyclotetradecane)†

Neil R. Champness,[a] Christopher S. Frampton,[b] Gillian Reid*,[a] and Derek A. Tocher[c]

[a] *Department of Chemistry, University of Southampton, Highfield, Southampton SO9 5NH, UK*

[b] *Roche Research Centre, Welwyn Garden City AL7 3AY, UK*

[c] *Department of Chemistry, University College London, Gordon Street, London WC1H 0AJ, UK*

The new diphosphadithia macrocycle 8,12-diphenyl-1,5-dithia-8,12-diphosphacyclotetradecane ($Ph_2[14]aneP_2S_2$) has been prepared and the *meso* isomer isolated as a white solid. Upon reaction with MCl_2 (M = Pd or Pt) in the presence of $TlPF_6$ in refluxing MeCN this isomer gave $[M(Ph_2[14]aneP_2S_2)][PF_6]_2$. The crystal structure of $[Pt(Ph_2[14]aneP_2S_2)][PF_6]_2 \cdot MeNO_2$ shows tetradentate P_2S_2 co-ordination at Pt^{II} giving a distorted square-planar geometry with Pt–P 2.247(3), 2.252(3) Å and Pt–S 2.343(3), 2.341(4) Å. Phosphorus-31 and ^{195}Pt NMR spectroscopic data confirm retention of this P_2S_2 co-ordination in solution. Treatment of $RhCl_3 \cdot 3H_2O$ with $Ph_2[14]aneP_2S_2$ in refluxing aqueous EtOH followed by addition of an excess of NH_4PF_6 gave $[RhCl_2(Ph_2[14]aneP_2S_2)]PF_6$ as a yellow solid. The ^{31}P NMR spectrum indicates that the complex exists as the *trans*-dichloro isomer exclusively, and a single-crystal X-ray structure determination confirms this. The crystal structure of $[RhCl_2(Ph_2[14]aneP_2S_2)]PF_6$ shows the macrocyclic donor atoms occupying the four equatorial co-ordination sites around the central Rh^{III} ion, Rh–P 2.286(1), 2.300(1) Å, Rh–S 2.374(1), 2.377(1) Å, with *trans*-dichloro ligands, Rh–Cl 2.347(1), 2.354(1) Å, giving a distorted octahedral geometry. Cyclic voltammetry shows that the complexes $[M(Ph_2[14]aneP_2S_2)][PF_6]_2$ (M = Pd or Pt) and *trans*-$[RhCl_2(Ph_2[14]aneP_2S_2)]PF_6$ each exhibit an irreversible reduction at E_{pc} values of −1.40, −1.93 and −1.06 V *vs.* ferrocene–ferrocenium respectively.

The co-ordination chemistry of phosphine ligands has been studied intensively and a vast number of mono- and bi-dentate phosphine complexes are known.[1] Interest in these has been stimulated largely by their catalytic properties which has led to several important industrial applications. In spite of this there have been relatively few systematic studies on macrocyclic phosphine chemistry.[2] This contrasts the now extensive chemistry of thioether and aza macrocycles, which are excellent ligands for both p- and d-block elements, forming highly stable species which are resistant to demetallation and often exhibit very unusual structural, electronic and redox properties.[3]

We have recently initiated a study aimed at establishing the effects upon the metal ion properties of placing phosphine functions together with S(thioether) or N(amine) donors in a macrocyclic environment. To this end, we are currently preparing a series of mixed phosphathia and phosphaaza macrocycles with a view to investigating their co-ordination to various metal ions.

Kyba *et al.*[4] have reported the preparations of several P_2E_2 (E = O, NR or S) and P_3S donor macrocycles all of which incorporate *o*-phenylene units in the backbone. These were found to act only as bidentate phosphine ligands to metal ions unless the ligand incorporated a 1-E-2-phosphinobenzo moiety. Another *trans*-P_2S_2 macrocycle has recently been reported by Wild and co-workers.[5] This was prepared in low yield *via* a Pt^{II}-template. The tetradentate P_2S_2 macrocycles chosen for our work involve a fully saturated backbone, thereby allowing greater conformational flexibility and a number of possible co-ordination modes. Some P_4E_2 (E = NR, O, S)[6] and PS_2[7] donor macrocycles having saturated backbones have been reported although their co-ordination chemistry has not yet been fully studied.

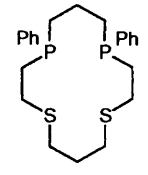

$Ph_2[14]aneP_2S_2$

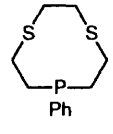

Ph[9]anePS_2

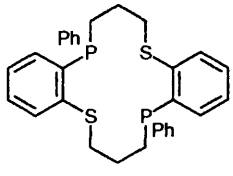

L^1

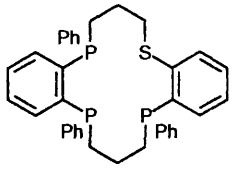

L^2

We now wish to report the synthesis of the mixed P_2S_2 donor macrocycle $Ph_2[14]aneP_2S_2$ and the quadridentate platinum metal macrocyclic complexes $[M(Ph_2[14]aneP_2S_2)][PF_6]_2$ (M = Pd or Pt) and *trans*-$[RhCl_2(Ph_2[14]aneP_2S_2)]PF_6$. The single-crystal structures of $[Pt(Ph_2[14]aneP_2S_2)][PF_6]_2 \cdot MeNO_2$ and *trans*-$[RhCl_2(Ph_2[14]aneP_2S_2)]PF_6$ are also presented.

Results and Discussion

The macrocycle $Ph_2[14]aneP_2S_2$ was prepared according to

† *Supplementary data available:* see Instructions for Authors, *J. Chem. Soc., Dalton Trans.*, 1994, Issue 1, pp. xxiii–xxviii.

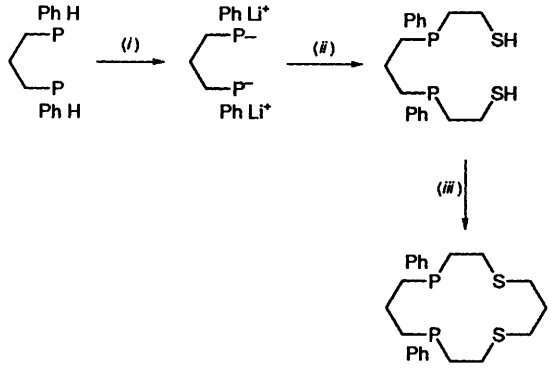

Scheme 1 (*i*) LiBu (2 equiv.)–thf; (*ii*) $(CH_2)_2S$ (2 equiv.) then MeOH–water; (*iii*) $Br(CH_2)_3Br$, Cs_2CO_3–dmf

Scheme 1 using a modification of the method reported by Blower and co-workers [7] for the preparation of Ph[9]anePS_2.[7] Thus, the disecondary phosphine $PhHP(CH_2)_3PHPh$ was treated with 2 molar equivalents of $LiBu^n$ and 2 molar equivalents of $(CH_2)_2S$ in tetrahydrofuran (thf) solution at −78 °C and hydrolysed with MeOH, to give the intermediate dithiol, $HS(CH_2)_2PPh(CH_2)_3PPh(CH_2)_2SH$. Cyclisation was then achieved by reaction of this dithiol with $BrCH_2CH_2CH_2Br$ at 65 °C over 24 h under high-dilution conditions in dimethylformamide (dmf)–Cs_2CO_3. This gave Ph_2[14]aneP_2S_2 as a light yellow oil obtained as a mixture of two stereoisomers. Subsequent treatment of this oil with acetone gave *meso*-Ph_2[14]aneP_2S_2 as a white solid (^{31}P NMR; δ −24.3, *m*/*z* = 421).

Reaction of MCl_2 (M = Pd or Pt) with 1 molar equivalent of *meso*-Ph_2[14]aneP_2S_2 in the presence of 2 molar equivalents of $TlPF_6$ in refluxing MeCN followed by addition of Et_2O yields pale yellow and white solids for M = Pd and Pt respectively. FAB mass spectrometry shows peaks at *m*/*z* 671, 525 and *m*/*z* 760, 614 with the correct isotopic distributions corresponding to $[Pd(Ph_2[14]aneP_2S_2)]PF_6^+$, $[Pd(Ph_2[14]aneP_2S_2 - H)]^+$ and $[Pt(Ph_2[14]aneP_2S_2)]PF_6^+$, $[Pt(Ph_2[14]aneP_2S_2 - H)]^+$ respectively. Together with IR, UV/VIS and ^{1}H NMR spectroscopic and microanalytical data, these results confirm the formulations $[M(Ph_2[14]aneP_2S_2)][PF_6]_2$ (M = Pd or Pt) for the products. The ^{31}P-{^{1}H} NMR spectrum (145.8 MHz, CD_3CN, 298 K) of $[Pd(Ph_2[14]aneP_2S_2)][PF_6]_2$ shows a singlet at δ +53.4 due to the macrocyclic P donors, as well as a septet at δ −146.6 due to the PF_6^- anions. For $[Pt(Ph_2[14]aneP_2S_2)][PF_6]_2$ ^{31}P-{^{1}H} NMR spectroscopy gives δ +46.2 with $^1J_{PtP}$ = 2718 Hz, and δ −145.8 (PF_6^- anion). The ^{31}P NMR resonances integrate as 1 : 1, confirming that only one macrocycle is ligated to each metal ion. Furthermore, in both systems a large downfield shift is observed upon co-ordination of Ph_2[14]aneP_2S_2. Such shifts are seen frequently where five-membered chelate rings occur, and hence are also consistent with P_2S_2 co-ordination to M^{II}.[8] The ^{195}Pt NMR spectrum (77.42 MHz, CD_3CN, 300 K) of $[Pt(Ph_2[14]aneP_2S_2)][PF_6]_2$ (Fig. 1) shows a triplet at δ −5174 ($^1J_{PtP}$ = 2718 Hz). This chemical shift is intermediate between those seen for S_4 and P_4 donor sets around Pt^{II}.[9]

To enable comparisons with other reported diphosphadithia macrocyclic systems a single-crystal structure determination was undertaken on $[Pt(Ph_2[14]aneP_2S_2)][PF_6]_2 \cdot MeNO_2$. Suitable crystals were grown by vapour diffusion of Et_2O into a solution of the complex in $MeNO_2$. The structure shows (Fig. 2) the macrocycle co-ordinated to the Pt^{II} ion in a tetradentate manner *via* two thioether and two phosphine donors, giving a distorted square-planar stereochemistry. Selected geometric parameters are listed in Table 1. The Ph groups are oriented on one side of the $Pt^{II}P_2S_2$ plane, with the methylene groups directed to the opposite side. The Pt^{II} ion is displaced above the least-squares P_2S_2 plane, towards the Ph rings, by 0.12 Å,

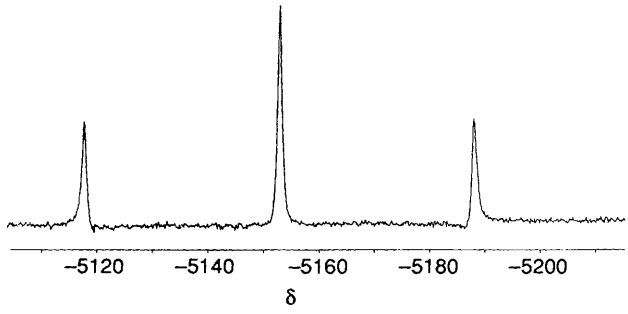

Fig. 1 Platinum-195 NMR spectrum of $[Pt(Ph_2[14]aneP_2S_2)][PF_6]_2$ (77.42 MHz, CD_3CN, 300 K)

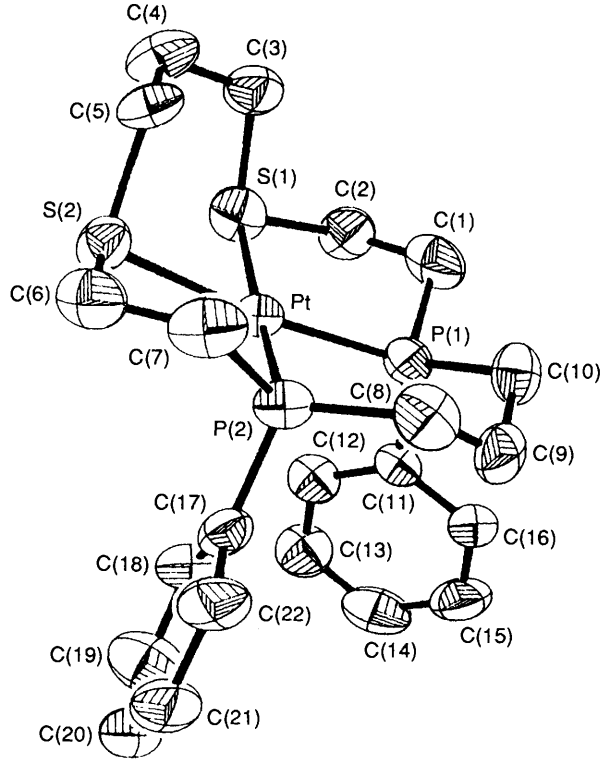

Fig. 2 View of the structure of $[Pt(Ph_2[14]aneP_2S_2)]^{2+}$ with numbering scheme adopted

indicating a rather poor size-match between the metal ion radius and the macrocyclic cavity. This contrasts with the structure of $[Pt([14]aneS_4)]^{2+}$ in which the Pt^{II} ion sits precisely in the least-squares S_4 co-ordination plane, Pt–S 2.271(3), 2.285(4), 2.301(3), 2.295(4) Å.[10] The Pt–P bond lengths in $[Pt(Ph_2[14]aneP_2S_2)]^{2+}$ are *ca.* 0.05 Å shorter and the Pt–S bond lengths *ca.* 0.05 Å longer than in $[PtL^1]^{2+}$, in which the P donors are *trans* to each other (Pt–P 2.300, 2.293, Pt–S 2.285, 2.294 Å).[4] In our complexes the thioether donors are *trans* to the phosphine donor atoms and these data strongly suggest a greater *trans* influence for P over S. A similar effect has been observed in the M–donor-atom bond lengths in $[PtL^2]^{2+}$, Pt–P(*trans* P) 2.289, 2.283 Å, Pt–P(*trans* S) 2.255 Å, Pt–S(*trans* P) 2.317 Å.[4]

We have also investigated the reaction between *meso*-Ph_2[14]aneP_2S_2 and the low-spin d^6 Rh^{III} metal ion. Reaction of $RhCl_3 \cdot 3H_2O$ with 1 molar equivalent of Ph_2[14]aneP_2S_2 in refluxing aqueous EtOH under N_2 affords a yellow solution and a brown precipitate. Addition of NH_4PF_6 to the filtered yellow solution gives the stable phosphathia macrocyclic complex $[RhCl_2(Ph_2[14]aneP_2S_2)]PF_6$ as an orange solid. The FAB mass spectrum of this species shows peaks with the correct isotopic distributions at *m*/*z* 593, 558 and 523, corresponding to $[^{103}Rh^{35}Cl_2(Ph_2[14]aneP_2S_2)]^+$ and successive loss of

Table 1 Selected bond lengths (Å), angles and torsion angles (°) for $[Pt(Ph_2[14]aneP_2S_2)]^{2+}$

Pt–P(1)	2.247(3)	C(4)–C(5)	1.547(18)	Pt–P(2)	2.252(3)	C(6)–C(7)	1.527(19)
Pt–S(1)	2.343(3)	C(8)–C(9)	1.523(20)	Pt–S(2)	2.341(4)	C(9)–C(10)	1.555(17)
P(1)–C(1)	1.824(14)	C(11)–C(12)	1.379(15)	P(1)–C(10)	1.801(12)	C(11)–C(16)	1.373(17)
P(1)–C(11)	1.798(11)	C(12)–C(13)	1.395(19)	P(2)–C(7)	1.812(16)	C(13)–C(14)	1.387(23)
P(2)–C(8)	1.825(13)	C(14)–C(15)	1.383(21)	P(2)–C(17)	1.787(11)	C(15)–C(16)	1.386(20)
S(1)–C(2)	1.826(14)	C(17)–C(18)	1.391(17)	S(1)–C(3)	1.824(14)	C(17)–C(22)	1.405(16)
S(2)–C(5)	1.827(12)	C(18)–C(19)	1.392(18)	S(2)–C(6)	1.850(14)	C(19)–C(20)	1.378(22)
C(1)–C(2)	1.527(18)	C(20)–C(21)	1.373(22)	C(3)–C(4)	1.525(22)	C(21)–C(22)	1.373(19)
P(1)–Pt–P(2)	94.2(1)	S(1)–C(3)–C(4)	111.5(9)	P(1)–Pt–S(1)	88.3(1)	C(3)–C(4)–C(5)	116.8(11)
P(2)–Pt–S(1)	173.7(1)	S(2)–C(5)–C(4)	111.6(9)	P(1)–Pt–S(2)	173.2(1)	S(2)–C(6)–C(7)	112.9(10)
P(2)–Pt–S(2)	87.8(1)	P(2)–C(7)–C(6)	109.6(9)	S(1)–Pt–S(2)	89.0(1)	P(2)–C(8)–C(9)	113.5(9)
Pt–P(1)–C(1)	103.9(5)	C(8)–C(9)–C(10)	115.1(11)	Pt–P(1)–C(10)	114.6(5)	P(1)–C(10)–C(9)	113.6(8)
C(1)–P(1)–C(10)	107.2(6)	P(1)–C(11)–C(12)	118.0(9)	Pt–P(1)–C(11)	113.7(4)	P(1)–C(11)–C(16)	122.7(8)
C(1)–P(1)–C(11)	108.2(6)	C(12)–C(11)–C(16)	119.3(11)	C(10)–P(1)–C(11)	108.8(6)	C(11)–C(12)–C(13)	121.3(12)
Pt–P(2)–C(7)	104.6(4)	C(12)–C(13)–C(14)	118.8(12)	Pt–P(2)–C(8)	116.8(4)	C(13)–C(14)–C(15)	119.9(14)
C(7)–P(2)–C(8)	105.8(6)	C(14)–C(15)–C(16)	120.2(14)	Pt–P(2)–C(17)	114.0(4)	C(11)–C(16)–C(15)	120.4(11)
C(7)–P(2)–C(17)	107.3(6)	P(2)–C(17)–C(18)	120.3(9)	C(8)–P(2)–C(17)	107.5(5)	P(2)–C(17)–C(22)	121.9(9)
Pt–S(1)–C(2)	104.2(4)	C(18)–C(17)–C(22)	117.8(11)	Pt–S(1)–C(3)	99.9(4)	C(17)–C(18)–C(19)	121.4(12)
C(2)–S(1)–C(3)	103.5(6)	C(18)–C(19)–C(20)	119.4(13)	Pt–S(2)–C(5)	97.9(5)	C(19)–C(20)–C(21)	119.7(13)
Pt–S(2)–C(6)	103.7(5)	C(20)–C(21)–C(22)	121.5(12)	C(5)–S(2)–C(6)	104.0(6)	C(17)–C(22)–C(21)	120.1(12)
P(1)–C(1)–C(2)	111.1(8)			S(1)–C(2)–C(1)	112.8(9)		

C(10)–P(1)–C(1)–C(2)	−167.2	P(2)–C(8)–C(9)–C(10)	70.5	C(12)–C(11)–C(16)–C(15)	−0.5
C(11)–P(1)–C(1)–C(2)	75.6	C(1)–P(1)–C(10)–C(9)	172.0	C(14)–C(15)–C(16)–C(11)	−0.7
C(3)–S(1)–C(2)–C(1)	78.3	C(11)–P(1)–C(10)–C(9)	−71.2	C(7)–P(2)–C(17)–C(18)	25.7
P(1)–C(1)–C(2)–S(1)	47.7	C(8)–C(9)–C(10)–P(1)	−75.2	C(7)–P(2)–C(17)–C(22)	−53.8
C(2)–S(1)–C(3)–C(4)	−178.2	C(1)–P(1)–C(11)–C(12)	−81.0	C(8)–P(2)–C(17)–C(10)	−20.8
S(1)–C(3)–C(4)–C(5)	73.2	C(1)–P(1)–C(11)–C(16)	97.7	C(8)–P(2)–C(17)–C(22)	59.5
C(6)–S(2)–C(5)–C(4)	180.0	C(10)–P(1)–C(11)–C(12)	162.8	P(2)–C(17)–C(18)–C(19)	79.5
C(3)–C(4)–C(5)–S(2)	−75.8	C(10)–P(1)–C(11)–C(16)	−18.4	C(22)–C(17)–C(18)–C(19)	−0.9
C(5)–S(2)–C(6)–C(7)	−75.4	P(1)–C(11)–C(12)–C(13)	179.1	C(17)–C(18)–C(19)–C(20)	3.8
C(8)–P(2)–C(7)–C(6)	171.6	C(16)–C(11)–C(12)–C(13)	0.4	C(18)–C(19)–C(20)–C(21)	−4.9
C(17)–P(2)–C(7)–C(6)	−73.8	C(11)–C(12)–C(13)–C(14)	0.9	C(19)–C(20)–C(21)–C(22)	3.2
S(2)–C(6)–C(7)–P(2)	−49.1	C(12)–C(13)–C(14)–C(15)	2.1	P(2)–C(17)–C(22)–C(21)	178.7
C(7)–P(2)–C(8)–C(9)	−166.8	C(13)–C(14)–C(15)–C(16)	1.9	C(18)–C(17)–C(22)–C(21)	−0.9
C(17)–P(2)–C(8)–C(9)	78.7	P(1)–C(11)–C(16)–C(15)	−179.2	C(20)–C(21)–C(22)–C(17)	−0.3

chlorine atoms from this species. This, together with IR and ^1H NMR spectroscopic and microanalytical data, confirms our assignment of the product as $[RhCl_2(Ph_2[14]aneP_2S_2)]PF_6$.

In order to verify the stereochemistry around Rh^{III} we undertook a single-crystal X-ray analysis. Suitable crystals were obtained by slow evaporation from a solution of the complex in CH_2Cl_2. The X-ray structure of $[RhCl_2(Ph_2[14]aneP_2S_2)]PF_6$ shows (Fig. 3) the cation adopting a *trans*-dichloro octahedral geometry, with the macrocyclic ligand occupying the four equatorial co-ordination sites in an up, up, up, up or *cccc* configuration, *i.e.*, as in the platinum(II) complex above, the methylene groups of the macrocycle all lie on one side of the RhP_2S_2 plane, with both phenyl substituents directed towards the opposite side of this plane. The Rh^{III} ion lies 0.08 Å above the least-squares P_2S_2 co-ordination plane towards the phenyl groups. The shorter Rh–P bond lengths (*cf.* Rh–S) are again consistent with the P-donors exhibiting a greater *trans* influence than the S-donors. There is a substantial steric interaction between the Ph groups and the adjacent Cl(2) atom, resulting in a tilting of Cl(2) from perpendicular [Cl–Rh–Cl 171.10(4)°]. The *trans*-dichloro stereochemistry observed for $[RhCl_2(Ph_2[14]aneP_2S_2)]^+$ markedly contrasts that seen for the analogous 14-membered tetrathia analogue $[RhCl_2([14]aneS_4)]^+$ which exists exclusively as the *cis*-dichloro isomer, with the thioether crown in a folded configuration, Rh–S 2.2870(12), 2.3275(12) Å, Rh–Cl 2.3836(12) Å.[11] This difference is surprising given the similarity in the covalent radii of P and S (1.10 and 1.04 Å respectively), and hence the similarity in the macrocyclic cavity size. The difference is presumably largely a consequence of the steric influence of the Ph substituents on the phosphine donors, together with the fact that unlike thioethers there is a high energy barrier to interconversion of the stereochemistries at the phosphines. The $^{31}P\text{-}\{^1H\}$ NMR spectrum of $[RhCl_2(Ph_2[14]aneP_2S_2)]PF_6$ measured at 300 K in MeCN solution shows, in addition to the septet at δ −146.0 from PF_6^-, a sharp doublet centred at δ +50.6. Coupling to ^{103}Rh is well resolved giving $^1J_{RhP} = 96$ Hz. The NMR spectroscopic data are consistent with the solid-state *trans*-dichloro stereochemistry being retained in solution.

The electronic spectrum of *trans*-$[RhCl_2(Ph_2[14]aneP_2S_2)]PF_6$ (MeCN solution) approximates to local D_{4h} symmetry with an intense band at $\lambda_{max} = 261$ nm ($\varepsilon_{mol} = 23\,430$ dm^3 mol^{-1} cm^{-1}) assigned to the $\pi \longrightarrow \pi^*$ transition within the Ph groups. Additionally two much weaker bands are apparent at $\lambda_{max} = 299$ (ε_{mol} *ca.* 7400, sh) and 410 nm (523 dm^3 mol^{-1} cm^{-1}), the latter corresponding to the $^1A_{1g} \longrightarrow {}^1E_g$ transition.

Cyclic voltammetric measurements on $[M(Ph_2[14]aneP_2S_2)][PF_6]_2$ in MeCN solution (0.1 mol dm^{-3} $NBu^n_4BF_4$ supporting electrolyte) show an irreversible reduction at $E_{pc} = -1.40$ and -1.93 V *vs.* ferrocene–ferrocenium respectively for M = Pd and Pt. These potentials are considerably more cathodic than for the corresponding tetrathia macrocyclic complexes $[M([14]aneS_4)]^{2+}$ ($E_{pc} = -0.90$ and -1.45 V *vs.* ferrocene–ferrocenium respectively for M = Pd and Pt).[12] The complex *trans*-$[RhCl_2(Ph_2[14]aneP_2S_2)]PF_6$ also exhibits an irreversible reduction at $E_{pc} = -1.06$ V *vs.* ferrocene–ferrocenium. The irreversibility may correspond to loss of Cl^- from a reduced rhodium(II) species. Similar behaviour has been observed for $[RhCl_2L]^+$, L = [12]-, [14]- and [16]-aneS$_4$ ($E_{pc} = -1.10$, -1.10 and -0.83 V *vs.* ferrocene–ferrocenium respectively).[11]

Conclusion

These results demonstrate that *meso*-$Ph_2[14]aneP_2S_2$ co-

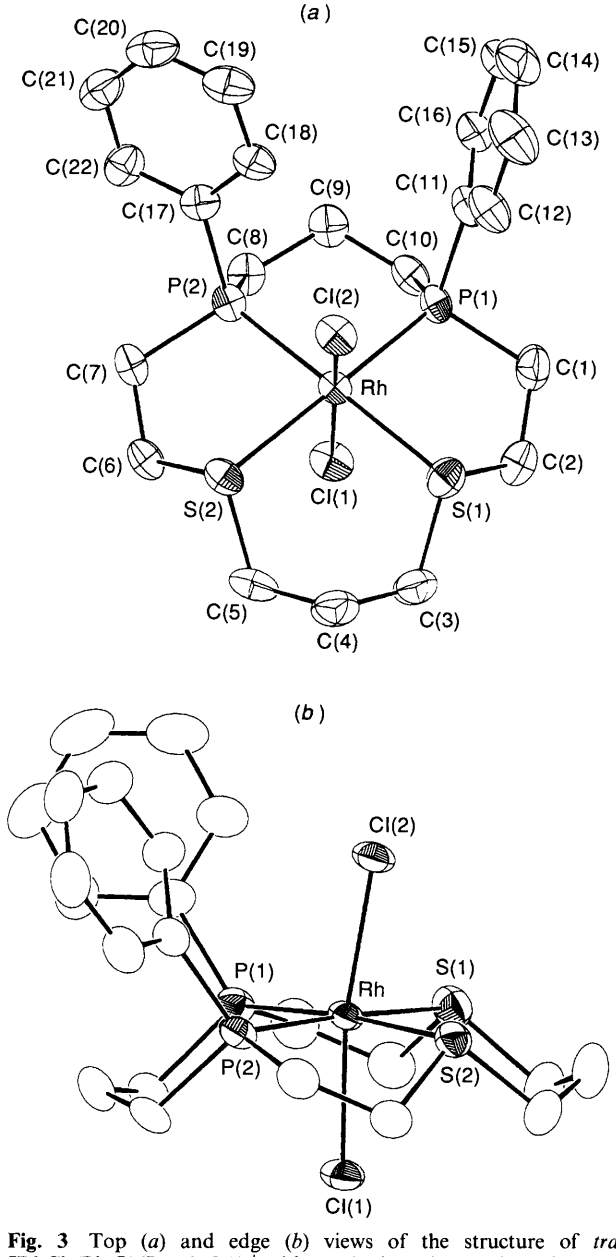

Fig. 3 Top (*a*) and edge (*b*) views of the structure of *trans*-$[RhCl_2(Ph_2[14]aneP_2S_2)]^+$ with numbering scheme adopted (H atoms have been omitted for clarity)

ordinates readily to platinum metal centres in an endocyclic arrangement involving co-ordination through a P_2S_2 donor set, and without any additional rigidity such as *o*-phenylene moieties in the macrocyclic backbone being necessary. Also, the generation of a *trans*-dichloro stereochemistry for $[RhCl_2(Ph_2[14]aneP_2S_2)]^+$ indicates that the substitution of thioether donors for phosphines in [14]aneS_4 leads to different co-ordinating properties, and hence possibly different reactivities.

We are currently investigating the ability of $Ph_2[14]aneP_2S_2$ to stabilise other oxidation states such as Rh^I, Ir^I, Pd^{IV} and Pt^{IV}, as well as synthesis of other P, S and P, N macrocyclic ligands and separation of the stereoisomers.

Experimental

Infrared spectra were measured as KBr or CsI discs or as Nujol mulls using a Perkin-Elmer 983 spectrometer over the range 200–4000 cm^{-1}. Mass spectra were run by electron impact or fast-atom bombardment (FAB) using 3-noba (3-nitrobenzyl alcohol) as matrix on a VG Analytical 70-250-SE normal geometry double focusing mass spectrometer. Solution UV/VIS spectra were recorded in 1 cm pathlength quartz cells using a Perkin-Elmer Lambda 19 spectrophotometer. Proton NMR spectra were recorded using a Bruker AM300 spectrometer. Phosphorus-31 NMR spectra were recorded using a Bruker AM360 spectrometer operating at 145.8 MHz and are referenced to 85% H_3PO_4 (δ 0). Platinum-195 NMR spectra were run using 10 mm diameter tubes containing 10–15% deuteriated solvent or a 5 mm insert tube of D_2O as a lock, on a Bruker AM360 spectrometer operating at 77.42 MHz and are referenced against a solution of Na_2PtCl_6 in H_2O (δ 0). Microanalyses were performed by the Imperial College microanalytical service. Cyclic voltammetric experiments were performed using an EG&G Princeton Applied Research Model 362 scanning potentiostat with 0.1 mol dm^{-3} $NBu^n_4BF_4$ supporting electrolyte, using a double platinum electrode as working and auxiliary electrode and a Ag–AgCl reference electrode. All potentials are quoted *versus* ferrocene–ferrocenium (for which $E_{\frac{1}{2}} = 0$ V).

All manipulations during the ligand preparation were performed using a dinitrogen atmosphere; thf was dried by distillation from sodium benzophenone under a N_2 atmosphere.

Synthesis.—$Ph_2[14]aneP_2S_2$. To a stirred solution of $PhHP(CH_2)_3PHPh$[13] (4.0 g, 0.015 mol) in thf (70 cm^3) was added dropwise $LiBu^n$ (0.032 mol, 1.3 mol dm^{-3} in hexane) generating a red solution of the phosphide. This solution was cooled to −78 °C (acetone slush) and a solution of $(CH_2)_2S$ (1.85 g, 0.03 mol) in thf (15 cm^3) was added dropwise over a period of 15 min. This mixture was allowed to warm to room temperature and was stirred for 30 min during which time the solution changed in colour from red to yellow. Methanol (40 cm^3) was then added causing formation of a white precipitate which redissolved upon addition of further MeOH. The mixture was then washed with water (40 cm^3) and the organic layer separated. The aqueous layer was washed with CH_2Cl_2 (2 × 15 cm^3) and the combined organic layers dried over $MgSO_4$. The drying agent was filtered off and the solvent removed under vacuum giving a yellow oil, $HS(CH_2)_2PPh(CH_2)_3PPh(CH_2)_2SH$, which was then washed with deoxygenated MeOH (20 cm^3).

The intermediate $HS(CH_2)_2PPh(CH_2)_3PPh(CH_2)_2SH$ (3.56 g, 9.4 mmol) was dissolved in dmf (300 cm^3) with $Br(CH_2)_3Br$ (1.90 g, 9.4 mmol) and this solution was added dropwise to a stirred suspension of Cs_2CO_3 (4.38 g, 0.013 mol) in dmf (1500 cm^3) at 65 °C, over a period of 24 h. The reaction was stirred for a further 2 h and then allowed to cool to room temperature. The dmf was distilled off under vacuum leaving a light yellow oil. This oil was washed with deoxygenated water (30 cm^3) to remove Cs_2CO_3. The resultant oil was redissolved in CH_2Cl_2 (15 cm^3) and deoxygenated acetone added dropwise to give *meso*-$Ph_2[14]aneP_2S_2$ as a white precipitate which was filtered using Schlenk apparatus and dried *in vacuo* (0.20 g, 5%, unoptimised). FAB mass spectrum (3-noba matrix): m/z = 421; calc. for $Ph_2[14]aneP_2S_2$ 420. ^{31}P-{^1H} NMR ($CDCl_3$, 298 K) (145.8 MHz), δ −24.3; ^1H (360 MHz), δ 7.2–7.4 (m, Ph, 10 H), 2.3–2.7 (m, PCH_2 and SCH_2, 16 H) and 1.8–2.0 (m, $CH_2CH_2CH_2$, 4 H).

$[Pd(Ph_2[14]aneP_2S_2)][PF_6]_2$.Palladium(II) chloride (22 mg, 0.12 mmol), $Ph_2[14]aneP_2S_2$ (50 mg, 0.12 mmol) and $TlPF_6$ (87 mg, 0.25 mmol) were refluxed in MeCN (30 cm^3) under a dinitrogen atmosphere for 3 h to give a yellow solution and white precipitate. The solution was then filtered to remove the TlCl and the volume reduced to *ca.* 5 cm^3 of MeCN. Diethyl ether was then added to give a yellow solid which was collected by filtration, recrystallised from acetone–MeOH and dried *in vacuo* (yield 71%) (Found: C, 31.6; H, 3.3. $C_{22}H_{30}F_{12}P_4PdS_2$ requires C, 32.40; H, 3.70%). FAB mass spectrum (3-noba matrix): m/z 671 and 525; calc. for $[^{106}Pd(Ph_2[14]aneP_2S_2)PF_6]^+$ 671, $[^{106}Pd(Ph_2[14]aneP_2S_2)]^+$ 526. UV/VIS spectrum (MeCN solution): λ_{max} 271 nm (ε_{mol} 16 530 dm^3 mol^{-1}

Table 2 Fractional atomic coordinates for $[Pt(Ph_2[14]aneP_2S_2)][PF_6]_2 \cdot MeNO_2$

Atom	x	y	z	Atom	x	y	z
Pt	4 783(1)	1 675(1)	1 928(1)	C(19)	2 067(11)	3 833(13)	711(9)
P(1)	4 378(2)	1 884(2)	3 008(2)	C(20)	2 109(11)	4 781(11)	426(7)
P(2)	4 949(2)	3 333(2)	1 743(2)	C(21)	2 992(13)	5 310(10)	571(1)
S(1)	4 801(2)	−64(2)	2 128(2)	C(22)	3 853(10)	4 898(8)	968(7)
S(2)	5 390(2)	1 387(2)	879(2)	P(3)	6 835(3)	6 750(3)	1 362(2)
C(1)	4 817(10)	734(11)	3 494(6)	F(1)	5 955(9)	7 455(8)	1 443(8)
C(2)	4 519(11)	−192(9)	3 024(7)	F(2)	7 086(10)	7 481(9)	791(8)
C(3)	6 145(10)	−300(10)	2 281(7)	F(3)	6 581(9)	5 997(9)	1 933(6)
C(4)	6 537(11)	−193(9)	1 589(8)	F(4)	6 116(9)	6 141(8)	764(6)
C(5)	6 617(9)	888(10)	1 303(7)	F(5)	7 697(8)	6 043(10)	1 257(7)
C(6)	5 666(10)	2 664(10)	585(7)	F(6)	7 582(11)	7 329(12)	1 939(8)
C(7)	5 901(10)	3 413(10)	1 206(8)	P(4)	9 033(2)	2 288(3)	658(2)
C(8)	5 398(9)	4 108(10)	2 537(7)	F(7)	8 947(8)	1 391(9)	1 178(6)
C(9)	4 821(10)	3 949(9)	3 134(7)	F(8)	9 187(9)	3 112(8)	89(6)
C(10)	5 002(10)	2 919(9)	3 527(7)	F(9)	9 441(12)	1 504(8)	173(8)
C(11)	3 053(8)	1 991(8)	2 964(6)	F(10)	7 948(7)	2 077(11)	243(6)
C(12)	2 418(9)	1 447(9)	2 442(7)	F(11)	10 121(7)	2 510(10)	1 070(7)
C(13)	1 382(10)	1 482(10)	2 382(8)	F(12)	8 581(15)	3 029(12)	1 119(9)
C(14)	992(10)	2 088(12)	2 851(9)	N(50)	2 438(14)	230(11)	512(8)
C(15)	1 630(12)	2 620(12)	3 383(8)	O(50)	3 220(14)	7(16)	339(10)
C(16)	2 658(9)	2 573(9)	3 434(6)	O(51)	2 182(17)	−18(12)	1 054(7)
C(17)	3 844(9)	3 915(8)	1 239(6)	C(50)	1 751(16)	794(12)	−16(10)
C(18)	2 940(9)	3 395(9)	1 097(7)				

Table 3 Selected bond lengths (Å), angles and torsion angles (°) for *trans*-$[RhCl_2(Ph_2[14]aneP_2S_2)]^+$

Rh–Cl(1)	2.347(1)	P(1)–C(11)	1.819(5)	Rh–Cl(2)	2.354(1)	P(2)–C(7)	1.849(4)
Rh–S(1)	2.377(1)	P(2)–C(8)	1.830(4)	Rh–S(2)	2.374(1)	P(2)–C(17)	1.820(4)
Rh–P(1)	2.300(1)	C(1)–C(2)	1.539(7)	Rh–P(2)	2.286(1)	C(3)–C(4)	1.529(8)
S(1)–C(2)	1.812(5)	C(4)–C(5)	1.519(8)	S(1)–C(3)	1.829(6)	C(6)–C(7)	1.512(7)
S(2)–C(5)	1.809(5)	C(8)–C(9)	1.533(6)	S(2)–C(6)	1.828(5)	C(9)–C(10)	1.536(7)
P(1)–C(1)	1.849(5)			P(1)–C(10)	1.819(4)		
Cl(1)–Rh–Cl(2)	171.10(4)	Rh–P(1)–C(10)	111.1(1)	Cl(1)–Rh–S(1)	88.22(4)	Rh–P(1)–C(11)	121.6(1)
Cl(1)–Rh–S(2)	88.04(4)	C(1)–P(1)–C(10)	109.0(2)	Cl(1)–Rh–P(1)	87.33(4)	C(1)–P(1)–C(11)	102.8(2)
Cl(1)–Rh–P(2)	88.18(4)	C(10)–P(1)–C(11)	105.4(2)	Cl(2)–Rh–S(1)	86.52(4)	Rh–P(2)–C(7)	106.8(2)
Cl(2)–Rh–S(2)	85.45(4)	Rh–P(2)–C(8)	111.6(2)	Cl(2)–Rh–P(1)	99.40(4)	Rh–P(2)–C(17)	122.9(2)
Cl(2)–Rh–P(2)	97.30(4)	C(7)–P(2)–C(8)	107.3(2)	S(1)–Rh–S(2)	96.65(4)	C(7)–P(2)–C(17)	103.7(2)
S(1)–Rh–P(1)	85.61(4)	C(8)–P(2)–C(17)	103.4(2)	S(1)–Rh–P(2)	175.89(4)	S(1)–C(2)–C(1)	109.5(3)
S(2)–Rh–P(1)	174.79(4)	P(1)–C(1)–C(2)	114.0(3)	S(2)–Rh–P(2)	85.20(4)	C(3)–C(4)–C(5)	115.0(5)
P(1)–Rh–P(2)	92.26(4)	S(1)–C(3)–C(4)	111.9(4)	Rh(1)–S(1)–C(2)	101.2(2)	S(2)–C(6)–C(7)	109.0(3)
Rh–S(1)–C(3)	108.3(2)	S(2)–C(5)–C(4)	111.7(4)	C(2)–S(1)–C(3)	100.8(2)	P(2)–C(8)–C(9)	113.8(3)
Rh–S(2)–C(5)	108.3(2)	P(2)–C(7)–C(6)	113.5(3)	Rh–S(2)–C(6)	100.7(1)	P(1)–C(10)–C(9)	114.9(3)
C(5)–S(2)–C(6)	101.0(2)	C(8)–C(9)–C(10)	117.1(4)	Rh–P(1)–C(1)	106.3(2)		

S(1)–C(2)–C(1)–P(1)	−45.3(4)	C(11)–C(12)–C(13)–C(14)	−1.7(10)	C(4)–C(5)–S(2)–C(6)	164.8(4)
P(1)–C(10)–C(9)–C(8)	−70.1(5)	C(12)–C(11)–C(16)–C(15)	−2.0(8)	C(6)–C(7)–P(2)–C(8)	103.0(3)
P(1)–C(11)–C(16)–C(15)	179.7(4)	C(13)–C(12)–C(11)–C(16)	3.0(8)	C(7)–P(2)–C(8)–C(9)	−177.2(3)
P(2)–C(17)–C(18)–C(19)	178.5(4)	C(17)–C(18)–C(19)–C(20)	−1.1(8)	C(7)–P(2)–C(17)–C(22)	−44.4(4)
C(1)–P(1)–C(10)–C(9)	176.8(3)	C(18)–C(17)–C(22)–C(21)	−0.6(7)	C(8)–P(2)–C(17)–C(22)	67.5(4)
C(1)–P(1)–C(11)–C(16)	110.5(4)	C(19)–C(18)–C(17)–C(22)	1.3(7)	C(9)–C(10)–P(1)–C(11)	−73.5(4)
C(2)–S(1)–C(3)–C(4)	−163.1(4)	S(1)–C(3)–C(4)–C(5)	64.1(5)	C(10)–P(1)–C(11)–C(16)	−3.6(5)
C(2)–C(1)–P(1)–C(11)	144.2(4)	P(1)–C(11)–C(12)–C(13)	−178.6(5)	C(11)–C(16)–C(15)–C(14)	−0.4(8)
C(5)–S(2)–C(6)–C(7)	−164.1(3)	P(2)–C(8)–C(9)–C(10)	69.8(5)	C(12)–C(13)–C(14)–C(15)	0(1)
C(6)–C(7)–P(2)–C(17)	−148.0(3)	P(2)–C(17)–C(22)–C(21)	−177.9(4)	C(13)–C(14)–C(15)–C(16)	1.8(10)
C(7)–P(2)–C(17)–C(18)	138.4(4)	C(1)–P(1)–C(11)–C(12)	−67.7(4)	C(17)–C(22)–C(21)–C(20)	−0.3(8)
C(8)–P(2)–C(17)–C(18)	−109.7(4)	C(1)–C(2)–S(1)–C(3)	162.8(4)	C(18)–C(19)–C(20)–C(21)	0.2(9)
C(9)–C(8)–P(2)–C(17)	73.6(4)	C(2)–C(1)–P(1)–C(10)	−104.4(4)	C(19)–C(20)–C(21)–C(22)	0.5(8)
C(10)–P(1)–C(11)–C(12)	178.1(4)				

cm^{-1}). NMR (300 K): ^1H (360 MHz, $CDCl_3$), δ 7.5–7.8 (m, Ph, 10 H), 3.5 (m), 3.1–3.3 (m), 2.8–3.0 (m) (all PCH_2 and SCH_2, 16 H) and 2.4 (br, $CH_2CH_2CH_2$, 4 H); ^{31}P-$\{^1H\}$ (145.8 MHz, MeCN), δ +53.4 (s, macrocyclic P, 2 P) and −146.6 (spt, PF_6^-, 2 P). IR spectrum (KBr disc): 3040w, 2980w, 2962w, 2840w, 1437m, 1420m, 1261m, 975m, 910w, 839vs br, 746m, 717m, 704w, 558vs, 490m, 473m and 396m cm^{-1}.

$[Pt(Ph_2[14]aneP_2S_2)][PF_6]_2$. Method as above, using $PtCl_2$ (34 mg, 0.13 mmol), $Ph_2[14]aneP_2S_2$ (54 mg, 0.13 mmol) and $TlPF_6$ (91 mg, 0.26 mmol). The product was isolated as a white solid (yield 50%) (Found: C, 26.9; H, 3.20%. $C_{22}H_{30}F_{12}P_4PtS_2 \cdot 2CH_2Cl_2$ requires C, 26.8; H, 3.20%). FAB mass spectrum (3-noba matrix): *m/z* 760 and 614; calc. for $[^{195}Pt(Ph_2[14]aneP_2S_2)PF_6]^+$ 760, $[^{195}Pt(Ph_2[14]aneP_2S_2)]^+$ 615. UV/VIS spectrum (MeCN solution): λ_{max} 260 nm (sh) (ε_{mol} *ca.* 3190 $dm^3\ mol^{-1}\ cm^{-1}$). NMR (300 K): ^1H (360 MHz, $CDCl_3$), δ 7.5–7.8 (m, Ph, 10 H), 3.7 (m), 3.2 (m), 3.0–2.7 (m) (PCH_2, SCH_2, 12 H) and 2.4 (br, $CH_2CH_2CH_2$, 4 H); ^{31}P-$\{^1H\}$ (145.8 MHz, CD_3CN), δ +46.2 (macrocyclic P, 2 P, $^1J_{PtP}$ = 2718 Hz) and −145.8 (spt, PF_6^-, 2 P); ^{195}Pt (77.4 MHz, MeCN), δ −5174 (t, $^1J_{PtP}$ = 2718 Hz). IR spectrum (KBr disc):

Table 4 Fractional atomic coordinates for *trans*-[$RhCl_2(Ph_2[14]aneP_2S_2)$]$PF_6$

Atom	*x*	*y*	*z*	Atom	*x*	*y*	*z*
Rh	0.264 55(2)	0.148 02(3)	0.958 56(2)	C(3)	0.218 6(4)	0.086 7(5)	0.785 7(3)
Cl(1)	0.107 55(8)	0.040 53(10)	0.942 97(6)	C(4)	0.313 4(5)	0.005 8(5)	0.793 1(3)
Cl(2)	0.431 02(8)	0.241 55(9)	0.958 69(6)	C(5)	0.309 1(4)	−0.075 0(4)	0.853 8(3)
S(1)	0.238 19(10)	0.209 4(1)	0.841 42(6)	C(6)	0.314 9(4)	−0.111 2(4)	0.998 2(3)
S(2)	0.365 08(8)	−0.014 42(9)	0.933 61(6)	C(7)	0.326 1(4)	−0.058 0(4)	1.069 5(3)
P(1)	0.155 25(8)	0.294 78(9)	0.986 33(6)	C(8)	0.145 2(3)	0.085 3(4)	1.110 6(2)
P(2)	0.276 83(8)	0.087 43(9)	1.071 50(6)	C(9)	0.090 5(4)	0.199 8(4)	1.112 9(2)
P(3)	0.843 9(1)	0.144 9(1)	0.718 65(8)	C(10)	0.049 9(3)	0.249 9(4)	1.043 0(3)
F(1)	0.881 2(3)	0.271 9(3)	0.724 7(2)	C(11)	0.209 9(4)	0.421 9(4)	1.025 6(3)
F(2)	0.808 0(3)	0.017 9(3)	0.714 8(2)	C(12)	0.296 0(4)	0.473 7(4)	0.993 4(3)
F(3)	0.865 5(8)	0.138 2(5)	0.802 6(3)	C(13)	0.341 8(5)	0.569 2(5)	1.022 0(4)
F(3a)	0.767(2)	0.149(2)	0.777(1)	C(14)	0.299 8(6)	0.615 0(5)	1.082 0(4)
F(4)	0.727 3(4)	0.185 4(7)	0.731 9(7)	C(15)	0.214 4(5)	0.568 0(4)	1.112 0(3)
F(4a)	0.745(2)	0.166(2)	0.663(1)	C(16)	0.167 7(4)	0.470 2(4)	1.084 5(3)
F(5)	0.828 6(9)	0.166 2(8)	0.640 3(3)	C(17)	0.363 6(3)	0.153 3(4)	1.138 2(2)
F(5a)	0.908(2)	0.108(1)	0.651(1)	C(18)	0.405 2(4)	0.260 7(4)	1.129 8(3)
F(6)	0.967 5(5)	0.119 0(6)	0.712 1(5)	C(19)	0.469 1(4)	0.306 7(5)	1.184 1(3)
F(6a)	0.930(2)	0.090(2)	0.762(2)	C(20)	0.489 7(4)	0.248 5(6)	1.245 3(3)
C(1)	0.092 5(4)	0.345 1(4)	0.903 1(3)	C(21)	0.447 6(4)	0.144 4(5)	1.253 3(3)
C(2)	0.101 9(4)	0.263 0(5)	0.842 1(3)	C(22)	0.385 5(4)	0.096 3(5)	1.200 9(3)

3020w, 2925w, 2860w, 1436m, 1420m, 1108m, 975m, 832vs br, 745m, 718m, 699m, 669w, 557vs, 505m, 493m, 475w, 453w cm^{-1}.

trans-[$RhCl_2(Ph_2[14]aneP_2S_2)$]$PF_6$. To a degassed solution of $RhCl_3 \cdot 3H_2O$ (0.03 g, 0.12 mmol) in EtOH (40 cm^3) and H_2O (1 cm^3) was added $Ph_2[14]aneP_2S_2$ (0.49 g, 0.12 mmol). Refluxing under a N_2 atmosphere for 1 h gave a yellow-brown solution. After cooling the solution was filtered yielding a brown solid. The yellow filtrate was treated with an excess of NH_4PF_6, the solvent removed and the product redissolved in CH_2Cl_2 (10 cm^3). This yellow solution was washed with H_2O (2 × 5 cm^3) to remove excess NH_4PF_6 and Et_2O added yielding a yellow precipitate (0.02 g, 23%) (Found: C, 34.6; H, 4.45. $C_{22}H_{30}Cl_2F_6P_3RhS_2 \cdot H_2O$ requires C, 34.9; H, 4.27%). FAB mass spectrum (3-noba matrix): *m/z* 593, 558, 523; calc. for $[^{103}Rh^{35}Cl_2(Ph_2[14]aneP_2S_2)]^+$ 593, $[^{103}Rh^{35}Cl(Ph_2[14]aneP_2S_2)]^+$ 558, $[^{103}Rh(Ph_2[14]aneP_2S_2)]^+$ 523. NMR (CD_3CN): ^1H (300 MHz), δ 7.1–7.6 (m, Ph, 10 H), 2.4–3.4 (m, PCH_2 and SCH_2, 16 H) and 1.8–2.1 (m, $CH_2CH_2CH_2$, 4 H); $^{31}P-\{^1H\}$ (145.8 MHz), δ 50.6 (d, $^1J_{RhP}$ = 96 Hz) and −146 (spt, PF_6^-). IR spectrum (KBr disc): 3020w, 2923w, 2870w, 1432m, 1420w, 1358w, 1261w, 1101m, 971w, 840vs br, 747m, 696m, 558vs, 508m and 448m cm^{-1}.

Crystallography.—*Structure determination on* [$Pt(Ph_2[14]aneP_2S_2)$][PF_6]$_2 \cdot MeNO_2$. Colourless crystals of the complex were obtained by vapour diffusion of diethyl ether into a solution of the complex in $MeNO_2$. The selected crystal (0.78 × 0.30 × 0.05 mm) was sealed in a glass capillary to prevent solvent loss.

Crystal data. $C_{22}H_{30}F_{12}P_4PtS_2 \cdot MeNO_2$, M = 966.7, monoclinic, space group $P2_1/n$, a = 13.649(5), b = 13.299(2), c = 18.983(7) Å, β = 101.89(3)°, U = 3372 $Å^3$ [from 2θ values of 30 reflections measured at ±ω (15 ⩽ 2θ ⩽ 26°, λ = 0.710 73 Å)], Z = 4, D_c = 1.90 g cm^{-3}, T = 293 K, μ = 4.60 mm^{-1}, $F(000)$ = 1888.

Data collection and processing. Nicolet R3mV four-circle diffractometer, graphite-monochromated Mo-Kα X-radiation, T = 293 K, ω–2θ scans, 6502 data collected, 5943 unique (R_{int} = 0.052) ($2\theta_{max}$ 50°, h 0 ⟶ 17, k 0 ⟶ 16, l −23 ⟶ 23) giving 4109 reflections with $F \geqslant 6\sigma(F)$ for use in all calculations. No significant crystal decay or movement was observed. The data were corrected for Lorentz and polarisation effects and empirically for absorption (max. and min. transmission factors = 0.98 and 0.36 respectively).

Structure solution and refinement. The structure was solved by direct methods and developed by using interative cycles of least-squares refinement and Fourier difference syntheses[14] which located all non-H atoms. The $[Pt(Ph_2[14]aneP_2S_2)]^{2+}$ cation, PF_6^- anions and $MeNO_2$ solvent molecule were all found to be ordered. All non-H atoms were refined anisotropically, while H-atoms were included in fixed, calculated positions (C–H = 0.96 Å) and assigned a common isotropic thermal parameter (U = 0.08 $Å^2$). The weighting scheme $w^{-1} = \sigma^2(F) + 0.001\,29F^2$ gave satisfactory agreement analyses. At final convergence R, R' = 0.0541, 0.0554 respectively, S = 1.45 for 406 refined parameters. The final ΔF synthesis showed two peaks above 1.5 e $Å^{-3}$ both of which lie close to the metal ion. Selected bond lengths, angles and torsion angles are given in Table 1. Fractional atomic coordinates are listed in Table 2.

Structure determination on [$RhCl_2(Ph_2[14]aneP_2S_2)$]$PF_6$. Orange crystals of the complex were obtained by slow evaporation from a solution of the complex in CH_2Cl_2. The selected crystal (0.20 × 0.08 × 0.45 mm) was mounted on a glass fibre.

Crystal data. $C_{22}H_{30}Cl_2F_6P_3RhS_2$, M = 739.3, monoclinic, space group $P2_1/c$, a = 12.431(2), b = 11.990(2), c = 19.206(1) Å, β = 92.437(9)°, U = 2860 $Å^3$ [from 2θ values of 25 reflections measured at ±ω (37.0 ⩽ 2θ ⩽ 39.9°, λ = 0.710 73 Å)], Z = 4, D_c = 1.72 g cm^{-3}, T = 294 K, μ(Mo-Kα) = 1.133 mm^{-1}, $F(000)$ = 1488.

Data collection and processing. Rigaku AFC7R four-circle diffractometer, graphite-monochromated Mo-Kα X-radiation, T = 294 K, ω–2θ scans, 6841 data collected, 6545 unique (R_{int} = 0.121), ($2\theta_{max}$ 54°, h 0 ⟶ 16, k 0 ⟶ 15, l −25 ⟶ 25) giving 4691 reflections with $F \geqslant 5\sigma(F)$ for use in all calculations. No significant crystal decay or movement was observed. The data were corrected for Lorentz and polarisation effects and as there were no measurable faces on the crystal the data were corrected empirically for absorption using ψ-scans (max. and min. transmission factors 0.999 and 0.856 respectively).

Structure solution and refinement. The structure was solved using heavy-atom Patterson methods.[15] Iterative cycles of least-squares refinement and Fourier difference synthesis revealed the positions of all non-H atoms for the one cation and PF_6^- anion in the asymmetric unit.[16] The structure was refined by full-matrix least squares, with anisotropic thermal parameters for all non-H atoms: H atoms were included but not refined. The PF_6^- anion was found to be disordered in one plane. This disorder was modelled by using partial F atom occupancies such that the P atom had a total of six F atoms around it, giving alternative F atom positions for F(3)–F(6). The weighting scheme $w^{-1} = \sigma^2(F)$ gave satisfactory agreement analyses. At final convergence, R, R' = 0.038, 0.043 respectively, S = 2.01 for 362 refined parameters. The final ΔF synthesis showed no peaks

above 0.78 or below -1.25 e $Å^{-3}$. Selected bond lengths, angles and torsion angles are given in Table 3. Fractional atomic coordinates are listed in Table 4.

Additional material available from the Cambridge Crystallographic Data Centre comprises H-atom coordinates, thermal parameters and remaining bond lengths and angles.

Acknowledgements

We thank the University of Southampton (N. R. C.) and SERC for support, and Johnson-Matthey plc for loans of platinum metal salts.

References

1 *The Chemistry of Organophosphorus Compounds*, ed. F. R. Hartley, Wiley, New York, 1990, vol. 1.
2 For examples, see D. J. Brauer, F. Gol, S. Hietkamp, H. Peters, H. Sommer, O. Stelzer and W. S. Sheldrick, *Chem. Ber.*, 1986, **119**, 349; E. P. Kyba and S.-T. Liu, *Inorg. Chem.*, 1985, **24**, 1613; B. N. Diel, R. C. Haltiwanger and A. D. Norman, *J. Am. Chem. Soc.*, 1982, **104**, 4700.
3 P. Chaudhuri and K. Wieghardt, *Prog. Inorg. Chem.*, 1987, **35**, 329; A. J. Blake and M. Schröder, *Adv. Inorg. Chem.*, 1990, **35**, 1; G. Reid and M. Schröder, *Chem. Soc. Rev.*, 1990, **19**, 239; S. R. Cooper and S. C. Rawle, *Struct. Bonding (Berlin)*, 1990, **72**, 1.
4 E. P. Kyba, R. E. Davis, C. W. Hudson, A. M. John, S. B. Brown, M. J. McPhaul, L.-K. Liu and A. C. Glover, *J. Am. Chem. Soc.*, 1981, **103**, 3868; E. P. Kyba, R. E. David, M. A. Fox, C. N. Clubb, S.-T. Liu, G. A. Reitz, V. J. Scheuler and R. P. Kashyap, *Inorg. Chem.*, 1987, **26**, 1647; E. P. Kyba, D. C. Alexander and A. Hohn, *Organometallics*, 1982, **1**, 1619; E. P. Kyba, C. N. Clubb, S. B. Larson, V. J. Scheuler and R. E. Davis, *J. Am. Chem. Soc.*, 1985, **107**, 2141.
5 T. L. Jones, A. C. Willis and S. B. Wild, *Inorg. Chem.*, 1992, **31**, 1411.
6 M. Ciampolini, P. Dapporto, A. Dei, N. Nardi and F. Zanobini, *Inorg. Chem.*, 1982, **21**, 489; M. Ciampolini, P. Dapporto, N. Nardi and F. Zanobini, *Inorg. Chem.*, 1983, **22**, 13; M. Ciampolini, N. Nardi, P. Dapporto, P. Innocenti and F. Zanobini, *J. Chem. Soc., Dalton Trans.*, 1984, 575; M. Ciampolini, N. Nardi, P. Dapporto and F. Zanobini, *J. Chem. Soc., Dalton Trans.*, 1984, 995; S. Mongani, P. Orioli, M. Ciampolini, N. Nardi and F. Zanobini, *Inorg. Chim. Acta*, 1984, **85**, 65; C. Mealli, M. Sabat, F. Zanobini, M. Ciampolini and N. Nardi, *J. Chem. Soc., Dalton Trans.*, 1985, 479.
7 R. J. Smith, A. K. Powell, N. Barnard, J. R. Dilworth and P. J. Blower, *J. Chem. Soc., Chem. Commun.*, 1993, 54.
8 P. Garrou, *Chem. Rev.*, 1981, **81**, 229.
9 See, for example, E. G. Hope, W. Levason and N. A. Powell, *Inorg. Chim. Acta*, 1986, **115**, 187.
10 D. Waknine, M. J. Heeg, J. F. Endicott and L. A. Ochrymowycz, *Inorg. Chem.*, 1991, **30**, 3691.
11 A. J. Blake, G. Reid and M. Schröder, *J. Chem. Soc., Dalton Trans.*, 1989, 1675.
12 A. J. Blake, A. J. Holder, G. Reid and M. Schröder, *J. Chem. Soc., Dalton Trans.*, 1994, 627, and unpublished work.
13 K. Sommer, *Z. Anorg. Allg. Chem.*, 1970, **376**, 37; B. R. Kimpton, W. McFarlane, A. S. Muir, P. G. Patel and J. L. Bookham, *Polyhedron*, 1993, **12**, 2525.
14 G. M. Sheldrick, SHELXTL PLUS, an integrated system for refining and displaying crystal structure from diffraction data, University of Göttingen, 1986.
15 P. T. Beurskens, G. Admiraal, G. Beurskens, W. P. Bosman, S. Garcia-Granda, R. O. Gould, J. M. M. Smits and C. Smykalla, PATTY, The DIRDIF program system, University of Nijmegen, 1992.
16 TEXSAN, Crystal Structure Analysis Package, Molecular Structure Corporation, Houston, TX, 1992.

Received 5*th July*, 1994; *Paper* 4/04111I